Cluster Compounds

Experimental and Theoretical Characterization of Superoxide Complexes [W$_2$O$_6$(O$_2^-$)] and [W$_3$O$_9$-(O$_2^-$)]: Models for the Interaction of O$_2$ with Reduced W Sites on Tungsten Oxide Surfaces**

Xin Huang, Hua-Jin Zhai, Tom Waters, Jun Li, and Lai-Sheng Wang**

High-valent transition-metal oxides (for example, V^V, Mo^{VI}, W^{VI}) are employed in a variety of important oxidation processes, and atmospheric dioxygen is commonly employed as a terminal oxidant.[1] Reoxidation of the metal oxide catalyst proceeds by a complex series of redox reactions, with the initial step generally assumed to be electron transfer from

[*] Dr. J. Li
W. R. Wiley Environmental Molecular Sciences Laboratory
Pacific Northwest National Laboratory, MS K1-96
P.O. Box 999, Richland, WA 99352 (USA)
Fax: (+1) 509-376-0420
E-mail: jun.li@pnl.gov

Dr. X. Huang, Dr. H.-J. Zhai, Dr. T. Waters, Prof. Dr. L.-S. Wang
Department of Physics
Washington State University
2710 University Drive, Richland, WA 99354 (USA)
and
W. R. Wiley Environmental Molecular Sciences Laboratory and
Chemical Sciences Division
Pacific Northwest National Laboratory, MS K8-88
P.O. Box 999, Richland, WA 99352 (USA)
Fax: (+1) 509-376-6066
E-mail: ls.wang@pnl.gov

a reduced metal site to dioxygen to form a bound superoxo complex.[2] Metal oxide clusters are being actively studied as model systems to obtain molecular-level information for surface and catalytic processes.[3,4] Herein we present a joint experimental and theoretical study of two O-rich tungsten oxide clusters, $[W_2O_8]^-$ and $[W_3O_{11}]^-$. Their electronic and geometric structures and chemical bonding were investigated by using photoelectron spectroscopy (PES) and density functional theory (DFT) calculations. The two anionic clusters are characterized as $[W_2O_6(O_2^-)]$ and $[W_3O_9(O_2^-)]$, respectively, that is, a superoxide species interacting with the neutral clusters $[W_2O_6]$ and $[W_3O_9]$ (chemisorption). In contrast, the neutral $[W_2O_8]$ and $[W_3O_{11}]$ clusters are found to contain an O_2 molecule weakly interacting with the $[W_2O_6]$ and $[W_3O_9]$ clusters (physisorption). The $[W_2O_8]^-$ and $[W_3O_{11}]^-$ clusters can be considered to be formed by non-dissociative electron transfer of the single W 5d electron in $[W_2O_6]^-$ and $[W_3O_9]^-$ to dioxygen (W 5d→O_2 π*) and are thus ideal molecular models for understanding the importance of reduced metal sites for the activation of O_2 on metal oxide nanostructures and surfaces.

The tungsten oxide clusters were produced by laser vaporization of a tungsten target in the presence of a helium carrier gas seeded with 0.5% O_2 and analyzed by using time-of-flight mass spectrometry.[5] Under the O_2-rich source conditions, clusters of the general formula $[W_nO_m]^-$ were formed, which appeared to terminate at the stoichiometry $[W_nO_{(3n+2)}]^-$ (n = 1–3) as shown in Figure 1. The mono-

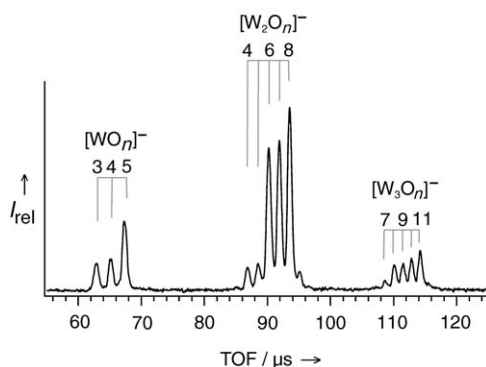**Figure 1.** Time-of-flight (TOF) mass spectrum of $[W_mO_n]^-$ clusters produced from laser vaporization of a pure tungsten target in a helium carrier gas containing 0.5% O_2.

tungsten species $[WO_n]^-$ (n = 2–5) and the ditungsten series $[W_2O_n]^-$ (n = 1–6) have been reported previously.[6,7] The present communication focuses on two O-rich clusters, $[W_2O_8]^-$ and $[W_3O_{11}]^-$. The photoelectron spectra of these two species recorded at 157 nm are compared with those of the two 1:3-stoichiometric clusters $[W_2O_6]^-$ and $[W_3O_9]^-$ in Figure 2. The spectra of the 1:3-stoichiometric species each exhibit a single, broad, low-binding-energy feature followed by a large energy gap. The low-binding-energy feature is due to detachment of the single W 5d electron in $[W_2O_6]^-$ and $[W_3O_9]^-$,[7,8] and its absence in the spectra of both $[W_2O_8]^-$ and $[W_3O_{11}]^-$ suggests that these clusters are formally W^{VI} d⁰ species. The spectra of the two O-rich clusters display
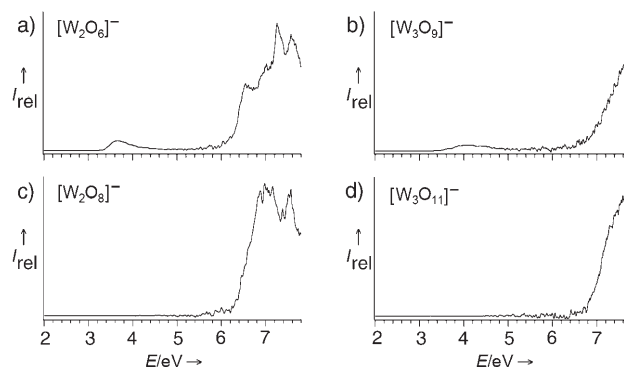

Figure 2. Photoelectron spectra of a) $[W_2O_6]^-$, b) $[W_3O_9]^-$, c) $[W_2O_8]^-$, and d) $[W_3O_{11}]^-$ recorded at 157 nm (7.866 eV).

broad detachment features with very high electron binding energies that are due to electron detachment from oxygen 2p orbitals. The detachment thresholds of $[W_2O_8]^-$ and $[W_3O_{11}]^-$ were estimated from the spectral onset of the first feature as about 6.4 and 6.9 eV, respectively. As shown below, there are large changes in the geometry between the anion and neutral ground states and these detachment thresholds do not represent the adiabatic detachment energies of $[W_2O_8]^-$ and $[W_3O_{11}]^-$.

The structure and bonding of the two clusters $[W_2O_6]^-$ and $[W_3O_9]^-$ have been described previously.[7,8] To obtain insight into the structure and bonding of $[W_2O_8]^-$ and $[W_3O_{11}]^-$ we carried out DFT calculations at the B3LYP level (see Methods Section). A variety of geometries for both the anions and their corresponding neutral species were tested and optimized to search for the global-minimum structures. The lowest-energy structures of the anions are shown in Figure 3 along with those of $[W_2O_6]^-$ and $[W_3O_9]^-$. A subset of the tested structures and their neutral species are given in

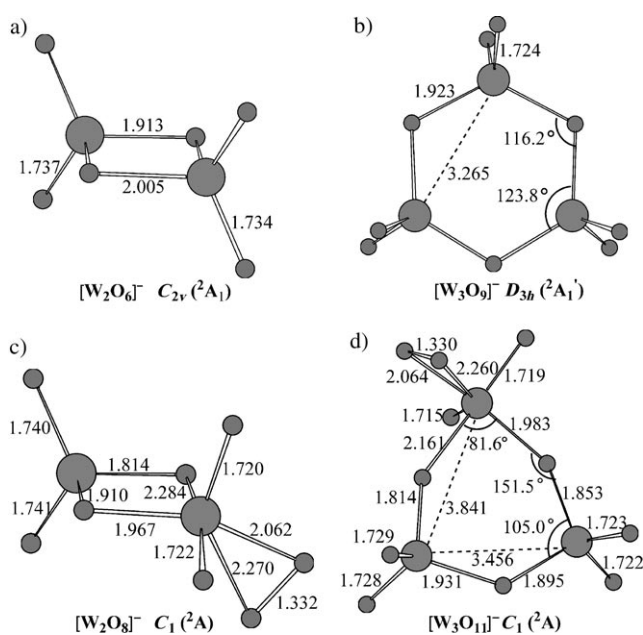**Figure 3.** Calculated ground-state structures for a) $[W_2O_6]^-$, b) $[W_3O_9]^-$, c) $[W_2O_8]^-$, and d) $[W_3O_{11}]^-$. Distances in Å.

the Supporting Information. The optimized structures for $[W_2O_8]^-$ and $[W_3O_{11}]^-$ with C_1 (^2A) symmetry bear some resemblance to those of $[W_2O_6]^-$ and $[W_3O_9]^-$, respectively, and can be viewed as the addition of an O_2 unit to one of the tungsten sites in the 1:3-stoichiometric clusters. The calculated O–O bond lengths of the O_2 units (1.33 Å) are very similar to that of the free superoxide (O_2^-) anion (1.34 Å at the B3LYP level), which suggests that these systems can be regarded as an O_2^- ion bound to neutral $[W_2O_6]$ and $[W_3O_9]$ clusters, respectively. The superoxide fragment is bound in an asymmetric, side-on fashion, with W–O bond lengths of 2.06 and 2.27 Å in $[W_2O_8]^-$ and 2.06 and 2.26 Å in $[W_3O_{11}]^-$ (Figure 3).

To gain further insight into the nature of the chemical bonding in the O-rich systems, we analyzed their valence molecular orbitals (MOs). The frontier orbitals of $[W_3O_{11}]^-$ are illustrated in Figure 4. The singly occupied MO is one of

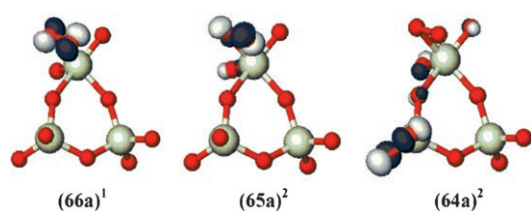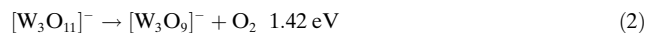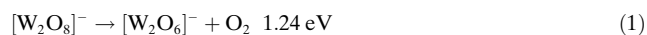**Figure 4.** Molecular orbital contour surfaces for the three highest-energy occupied orbitals of $[W_3O_{11}]^-$.

the two π^* orbitals of the bound O_2 unit, and the highest-energy doubly occupied MO is the second π^* orbital of O_2 that is singly occupied in free O_2. This orbital occupation is consistent with the O–O bond length described above and supports the description of $[W_3O_{11}]^-$ as an O_2^- unit bound to the neutral $[W_3O_9]$. The remaining valence MOs are all derived from oxygen 2p orbitals on the terminal and bridging oxo ligands (see, for example, 64a in Figure 4). The valence MOs of $[W_2O_8]^-$ and its chemical bonding are qualitatively similar to those of $[W_3O_{11}]^-$.

The optimized structures of the $[W_2O_8]$ and $[W_3O_{11}]$ neutral clusters (see Supporting Information) are dramatically different. In particular, the calculations predict a large increase in the separation between the O_2 fragment and the tungsten site; the calculated W–O distances increase from 2.06 and 2.27 Å in $[W_2O_8]^-$ to 2.67 and 3.49 Å in neutral $[W_2O_8]$, and from 2.06 and 2.26 Å in $[W_3O_{11}]^-$ to 3.83 and 4.57 Å in $[W_3O_{11}]$. Furthermore, the O–O length in the O_2 unit is reduced from 1.33 Å in the anions to 1.20 Å in the neutral species, which is very close to that of free O_2 (1.21 Å at the B3LYP level). These results suggest that removal of an electron from the doubly occupied π^* orbital of the O_2^- moiety significantly weakens the interaction of O_2 with $[W_2O_6]$ and $[W_3O_9]$, and that $[W_2O_8]$ and $[W_3O_{11}]$ are best described as O_2 physisorption onto $[W_2O_6]$ and $[W_3O_9]$, respectively. It should be pointed out that the weak interaction between O_2 and $[W_2O_6]$ or $[W_3O_9]$ means that the W–O_2 distances in these species calculated by using B3LYP should only be considered qualitatively, as such weak interactions are known to be poorly described by DFT

methods.[9] However, the effect of slight changes in these bond lengths on the exact geometry of O_2 in the neutral clusters should not alter the interpretation of the results, and the qualitative conclusions from these calculations are expected to be reliable.

The calculated vertical detachment energies (VDEs) for $[W_2O_8]^-$ and $[W_3O_{11}]^-$ are 6.40 and 6.88 eV, respectively, which are in reasonable agreement with the experimental data (Figure 2). However, the theoretical adiabatic detachment energies of 4.68 and 4.44 eV for $[W_2O_8]^-$ and $[W_3O_{11}]^-$, respectively, are significantly smaller than the corresponding VDEs because of the large structural changes between the ground states of the anions and the neutral species. These results are consistent with the broad photoelectron spectral features shown in Figure 2, which indicates that the experimental threshold values do not represent the adiabatic detachment energies of $[W_2O_8]^-$ and $[W_3O_{11}]^-$ and only represent their upper limits. As shown below, electron detachments involving the O_2^- orbitals from $[W_2O_8]^-$ and $[W_3O_{11}]^-$ are essentially dissociative detachments ($[W_2O_8]^- \rightarrow [W_2O_6] + O_2 + e^-$; $[W_3O_8]^- \rightarrow [W_3O_9] + O_2 + e^-$) because of the weak interaction between the neutral W_2O_6 and W_3O_9 clusters and O_2. VDEs for higher-binding-energy detachment channels were also computed and are shown in the Supporting Information; each VDE was fitted with a Gaussian function of 0.04-eV width to approximately simulate the photoelectron spectra.

To further understand the nature of interactions in $[W_2O_8]^-$ and $[W_3O_{11}]^-$, we computed the dissociation energies for the removal of the O_2 molecule [Eqs. (1) and (2)].[10]

$$[W_2O_8]^- \rightarrow [W_2O_6]^- + O_2 \quad 1.24 \text{ eV} \tag{1}$$

$$[W_3O_{11}]^- \rightarrow [W_3O_9]^- + O_2 \quad 1.42 \text{ eV} \tag{2}$$

The reverse of Equations (1) and (2) can be viewed as the reactions of O_2 with the anionic clusters. The presence of the extra 5d electrons in the $[W_2O_6]^-$ and $[W_3O_9]^-$ ions makes them susceptible to reaction with O_2 through transfer of one electron to O_2 to form the $[W_2O_6(O_2^-)]$ and $[W_3O_9(O_2^-)]$ superoxide complexes, respectively. This result is consistent with the nature of the frontier orbitals in $[W_2O_8]^-$ and $[W_2O_{11}]^-$ (Figure 4), which suggests that the interactions between $[W_2O_6]$ or $[W_3O_9]$ and O_2^- are mainly electrostatic. Conversely, the neutral clusters have extremely weak interactions with O_2 (calculated as < 0.1 eV in both cases) and essentially only form physisorbed $[W_2O_6(O_2)]$ and $[W_3O_9(O_2)]$ van der Waals complexes.[9] This behavior illustrates the importance of electrostatic interactions in the anionic species. In contrast, the O_2 interaction with the smallest 1:3-stoichiometric, neutral $[WO_3]$ cluster is quite different. We showed previously that O_2 and $[WO_3]$ form a charge-transfer complex $[(WO_3^+)(O_2^-)]$ as a result of the low coordination number of W in the C_{3v}-symmetric $[WO_3]$ monomer.[6]

The anionic clusters $[W_2O_6(O_2^-)]$ and $[W_3O_9(O_2^-)]$ can be considered as molecular models for the activation of O_2 through electron transfer between a reduced metal site and dioxygen at a metal oxide surface to form a coordinated

superoxide species.[2] The present work demonstrates this phenomenon at the molecular level in two model systems. In contrast, the absence of the W 5d electron in the neutral $[W_2O_6]$ and $[W_3O_9]$ clusters leads to physisorbed O_2 in $[W_2O_8]$ and $[W_3O_{11}]$, which can be compared to O_2 interacting with perfect $[WO_3]$ surfaces.

Methods Section

Photoelectron spectroscopy: The photodetachment experiments were carried out by using a magnetic-bottle PES apparatus equipped with a laser-vaporization supersonic-cluster source.[5] Briefly, the $[W_mO_n]^-$ cluster anions were produced by laser vaporization of a pure tungsten target in the presence of helium carrier gas seeded with 0.5% O_2 and were analyzed by using a time-of-flight mass spectrometer. The $[W_2O_8]^-$ and $[W_3O_{11}]^-$ species of current interest were mass-selected and decelerated before being photodetached by a laser beam of wavelength 157 nm (7.866 eV) from an F_2 excimer laser. Photoelectrons were collected at nearly 100% efficiency by the magnetic bottle and analyzed in a 3.5-m long electron flight tube. Photoelectron spectra were calibrated by using the known spectrum of Rh^-, and the energy resolution of the apparatus was $\Delta E_k/E_k \approx 2.5\%$, that is, ca. 25 meV for 1-eV electrons.

Theoretical calculations: The theoretical calculations were performed by using the hybrid DFT method B3LYP.[11] Geometries were optimized by using analytical energy gradients, and vibrational frequency calculations were performed to verify the nature of the stationary points. The Stuttgart 14-valence-electron relativistic pseudopotentials and the (8s7p6d)/(6s5p3d) valence basis sets augmented with two f- and one g-type polarization functions ($\zeta(f) = 0.256, 0.825; \zeta(g) = 0.627$) were used for tungsten,[12] and the aug-cc-pVTZ basis set was used for oxygen.[13] Vertical detachment energies (VDEs) were calculated by using a combined ΔSCF-TDDFT approach.[14] In this approach, the ground-state energies of the anions and the neutral species were calculated from the ΔSCF energy difference at the B3LYP level, whereas the excited states of the electron-detached species were obtained from TDDFT calculations of the neutral species. The dissociation energies were calculated as the total energy differences of the relevant species at their ground-state structures. Calculations were carried out by using the NWChem 4.6 program at the Molecular Science Computing Facility located at the Environmental Molecular Sciences Laboratory.[15] Three-dimensional contours of the calculated Kohn–Sham orbitals were generated with the Extensible Computational Chemistry Environment (Ecce) software package.[16]

[1] *Handbook of Heterogeneous Catalysis* (Eds.: G. Ertl, H. Knözinger, J. Weitkamp), Wiley, Weinheim, **1997**, pp. 2541.

[2] a) M. Che, A. J. Tench, *Adv. Catal.* **1983**, *32*, 1; b) K. Dyrek, M. Che, *Chem. Rev.* **1997**, *97*, 305; c) E. Giamello, *Catal. Today* **1998**, *41*, 239; d) M. Anpo, M. Che, B. Fubini, E. Garrone, E. Giamello, M. C. Paganini, *Top. Catal.* **1999**, *8*, 189; e) M. Labanowska, *ChemPhysChem* **2001**, *2*, 712; f) O. Diwald, E. Knözinger, *J. Phys. Chem. B* **2002**, *106*, 3495; g) T. Berger, M. Sterrer, O. Diwald, E. Knözinger, D. Panayotov, T. L. Thompson, J. T. Yates, Jr., *J. Phys. Chem. B* **2005**, *109*, 6061.

[3] For recent reviews see: a) D. K. Böhme, H. Schwarz, *Angew. Chem.* **2005**, *117*, 2388; *Angew. Chem. Int. Ed.* **2005**, *44*, 2336;

b) T. M. Bernhardt, *Int. J. Mass Spectrom.* **2005**, *243*, 1; c) K. A. Zemski, D. R. Justes, A. W. Castleman, Jr., *J. Phys. Chem. B* **2002**, *106*, 6136.

[4] For selected examples see: a) J. Döbler, M. Pritzsche, J. Sauer, *J. Am. Chem. Soc.* **2005**, *127*, 10861; b) G. Fu, X. Xu, X. Lu, H. L. Wan, *J. Am. Chem. Soc.* **2005**, *127*, 3989; c) M. L. Kimble, A. W. Castleman, Jr., R. Mitrić, C. Bürgel, V. Bonačić-Koutecký, *J. Am. Chem. Soc.* **2004**, *126*, 2526; d) T. Waters, R. A. J. O'Hair, A. G. Wedd, *J. Am. Chem. Soc.* **2003**, *125*, 3384; e) X. Xu, F. Faglioni, W. A. Goddard III, *J. Phys. Chem. A* **2002**, *106*, 7171; f) A. Muller, R. Maiti, M. Schmidtmann, H. Bogge, S. K. Das, W. J. Zhang, *Chem. Commun.* **2001**, 2126; g) Q. Sun, B. K. Rao, P. Jena, D. Stolcic, Y. D. Kim, G. Gantefor, A. W. Castleman, Jr., *J. Chem. Phys.* **2004**, *121*, 9417; h) B. L. Yoder, J. T. Maze, K. Raghavachari, C. C. Jarrold, *J. Chem. Phys.* **2005**, *122*, 094313.

[5] a) L. S. Wang, H. S. Cheng, J. Fan, *J. Chem. Phys.* **1995**, *102*, 9480; b) L. S. Wang, H. Wu in *Advances in Metal and Semiconductor Clusters. IV. Cluster Materials* (Ed.: M. A. Duncan), JAI, Greenwich, CT, **1998**, pp. 299–343.

[6] H. J. Zhai, B. Kiran, L. F. Cui, X. Li, D. A. Dixon, L. S. Wang, *J. Am. Chem. Soc.* **2004**, *126*, 16134.

[7] H. J. Zhai, X. Huang, L. F. Cui, X. Li, J. Li, L. S. Wang, *J. Phys. Chem. A* **2005**, *109*, 6019.

[8] X. Huang, H. J. Zhai, B. Kiran, L. S. Wang, *Angew. Chem.* **2005**, *117*, 7417; *Angew. Chem. Int. Ed.* **2005**, *44*, 7251.

[9] a) K. Müller-Dethlefs, P. Hobza, *Chem. Rev.* **2000**, *100*, 143; b) R. van Leeuwen, E. J. Baerends, *Phys. Rev. A* **1994**, *49*, 2421.

[10] The $[W_2O_8]^-$ and $[W_3O_{11}]^-$ ions also have another dissociation pathway to release O_2^- with much higher dissociation energies of 4.20 and 3.92 eV, respectively. The difference between this pathway and the O_2 pathway lies in the difference between the electron affinities of O_2 and the $[W_2O_6]$ and $[W_3O_9]$ clusters.

[11] a) A. D. Becke, *J. Chem. Phys.* **1993**, *98*, 1372; b) C. Lee, W. Yang, R. G. Parr, *Phys. Rev. B* **1988**, *37*, 785; c) P. J. Stephens, F. J. Devlin, C. F. Chabalowski, M. J. Frisch, *J. Phys. Chem.* **1994**, *98*, 11623.

[12] a) D. Andrae, U. Haeussermann, M. Dolg, H. Stoll, H. Preuss, *Theor. Chim. Acta* **1990**, *77*, 123; b) W. Küchle, M. Dolg, H. Stoll, H. Preuss, *Pseudopotentials of the Stuttgart/Dresden Group 1998* Revision Aug 11, 1998 (http://www.theochem.uni-stuttgart.de/pseudopotentiale); c) J. M. L. Martin, A. Sundermann, *J. Chem. Phys.* **2001**, *114*, 3408.

[13] a) T. H. Dunning, Jr., *J. Chem. Phys.* **1989**, *90*, 1007; b) R. A. Kendall, T. H. Dunning, Jr., R. J. Harrison, *J. Chem. Phys.* **1992**, *96*, 6796.

[14] a) J. Li, X. Li, H. J. Zhai, L. S. Wang, *Science* **2003**, *299*, 864; b) X. Li, B. Kiran, J. Li, H. J. Zhai, L. S. Wang, *Angew. Chem.* **2002**, *114*, 4980; *Angew. Chem. Int. Ed.* **2002**, *41*, 4786.

[15] "NWChem, A Computational Chemistry Package for Parallel Computers, Version 4.6" (2004), Pacific Northwest National Laboratory, Richland, Washington 99352-0999, USA. See Supporting Information.

[16] Extensible Computational Chemistry Environment (Ecce). http://ecce.emsl.pnl.gov/.